Journal of Food and Drug Analysis

Volume 32 | Issue 3 Article 2

Functional gold nanoparticles for analysis and delivery of nucleic acids

REVIEW ARTICLE

Functional gold nanoparticles for analysis and delivery of nucleic acids

Po-Tsang Huang [a,b], Yen-Ling Chen [a,c,d], Yi-Hui Lin [f], Chun-Chi Wang [a,e,g,**], Huan-Tsung Chang [h,i,j,k,*]

[a] School of Pharmacy, College of Pharmacy, Kaohsiung Medical University, Kaohsiung 807378, Taiwan
[b] Division of Pharmacy, Kaohsiung Armed Forces General Hospital, Kaohsiung 802301, Taiwan
[c] Department of Chemistry and Biochemistry, National Chung Cheng University, Chia-Yi 621301, Taiwan
[d] Department of Fragrance and Cosmetic Science, College of Pharmacy, Kaohsiung Medical University, Kaohsiung 807378, Taiwan
[e] Drug Development and Value Creation Research Center, Kaohsiung Medical University, Kaohsiung 807378, Taiwan
[f] School of Pharmacy, China Medical University, Taichung 406040, Taiwan
[g] Department of Medical Research, Kaohsiung Medical University Hospital, Kaohsiung 807378, Taiwan
[h] Department of Biomedical Sciences, Chang Gung University, Taoyuan 33302, Taiwan
[i] Graduate Institute of Biomedical Sciences, Chang Gung University, Taoyuan 33302, Taiwan
[j] Center for Advanced Biomaterials and Technology Innovation, Chang Gung University, Taoyuan 33302, Taiwan
[k] Division of Breast Surgery, Department of General Surgery, Chang Gung Memorial Hospital, Linkou, Taoyuan 33305, Taiwan

Abstract

Gold nanoparticles (AuNPs) have become the rising stars in the field of nanotechnology and made a revolution in exploiting the profundity of genomics due to their distinguished properties such as stability, ease in preparation and conjugation, biocompatibility, and unique optical properties. These characteristics have greatly expanded their applications such as sensitive and selective quantitation of nucleic acids and as effective carriers for specifically delivering various important molecules/biomolecules to various targets, which are the cornerstone in treating genetic disorders. This review comprehensively discusses the most recent progress in utilization of AuNPs in quantitation and delivery of nucleic acids. The future prospects and challenges of various methods have also been illustrated. It is believed that researchers will continue to overcome the limitations in previous approaches and AuNPs will still play vital roles in the development of diagnosis and treatment of gene-related diseases.

Keywords: DNA, Gene delivery, Gene quantitation, Gold nanoparticles, RNA

1. Introduction

Gold nanoparticles (AuNPs) are unique nanomaterials with controllable physiochemical properties, which have captured massive attention from biomedical experts. These properties include chemical stability, biocompatibility, localized surface plasmon resonance (LSPR) absorption and flexibility in surface functionalization. The chemical stability and biocompatibility made them suitable for numerous biological studies. Their ability to couple with many functional molecules increase their biofunctionality in addition to enhanced stability in complicated environments. Their unique LSPR properties allow them to outperform in biosensing, labelling and bioimaging [1]. Moreover, AuNPs can be assembled homogenously or heterogeneously, which results in more distinctive properties that diversify its applications in nanotechnology [2].

Various sizes and morphologies of AuNPs can be simply prepared by carefully controlling important factors such as reducing strength/concentration of reductant, molar ratio of reductant/gold ion, pH, temperature, and surfactant [3]. Through strong Au−S or Au−N bonding, various recognition elements like nucleic acids can be easily conjugated with AuNPs to prepare functional nanomaterials.

Received 26 March 2024; accepted 31 May 2024.
Available online 13 September 2024

* Corresponding author at: Department of Biomedical Sciences, Chang Gung University, Taiwan.
** Corresponding author at: School of Pharmacy, College of Pharmacy, Kaohsiung Medical University, 100, Shi-Chuan 1st Rd., Kaohsiung 807, Taiwan.
E-mail addresses: chunchi0716@kmu.edu.tw (C.-C. Wang), changht@mail.cgu.edu.tw (H.-T. Chang).

https://doi.org/10.38212/2224-6614.3514

For example, we are pioneers in conjugation of AuNPs with nucleic acids to prepare functional AuNPs for sensitive and selective detection of proteins [4] and for controlling the catalytic activity of thrombin [5]. Having photodynamic and photothermal activities, AuNPs conjugated with various recognition elements have been shown potential drugs for various diseases like cancer [6].

Nowadays, many diseases have been found to be identifiable with certain genes and their ways of expression. Some of them have even been validated to be curable with gene-mediated therapy, such as cancer, hepatitis, tuberculosis and Alzheimer's diseases [7]. However, traditional methods for nucleic acid analysis such as high-performance liquid chromatography-mass spectrometry (HPLC-MS) is rather unaffordable and time-consuming. Common gene delivery materials such as liposomes are encountered with obstacles like enzyme degradation and opsonization. Hence, precise quantitation and timely delivery of nucleic acids to sites of lesions become fundamental to early diagnosis and effective management of these diseases [8].

Supported by their favorable characteristics, exceptional advancements have been made in both quantitation and delivery of nucleic acids with AuNPs. For instance, over the past few years, point-of-care diagnostics of COVID-19 have become successful thanks to rapid and sensitive detection achieved with AuNPs [9]. A plethora of analytical methods and sensing platforms using AuNPs for identification of SARS-CoV-2 virus have been developed. In 2021, a colorimetric method for the detection of SARS-CoV-2 RNA derived from gold nanoparticle-core spherical nucleic acids (AuNP-core SNAs) has been developed, in which RNA was determined by the color change generated from inhibition of SNAs assembly caused by the cleavage of a palindromic linker [10]. Colorimetric detection of SARS-CoV-2 RNA was also conducted with the assistance of magnetic pull-down based on the CRISPR/Cas12a system. The presence of RNAs could be recognized by naked eye through hybridization with red DNA-AuNP probe, while the absence of RNA leaved the supernatant colorless as free DNA-AuNP probes were magnetically pulled down to the bottom of the test tube [11]. These novel discoveries were not only feasible in laboratories but also instrumental in controlling the spread of pandemic, which makes significant contribution to global health. In addition to that, through appropriate surface modification and functionalization, AuNPs can act as biomarkers for breast cancer by accurately binding to other biomolecules. These methods lead to meaningful progress in early discovery, prognosis evaluation and risk prediction of breast cancer, which offers us new insights into cancerous diseases [12].

Apart from quantitation of nucleic acids, gene delivery is also an area where AuNPs have been extensively used. AuNPs have been considered as promising carriers of genetic materials and distinguished tool in gene therapy. The functionalization of AuNPs and their bioconjugation with other organisms are commonly facilitated through strong Au−S or Au−N bonding [13]. The well-fabricated nanostructures of AuNPs sufficiently deliver genes to target sites and promote gene-silencing and gene-editing as effective treatments for genetic disorders, including Duchene's muscular dystrophy and autism [14]. It has also been highlighted by many studies that AuNPs are trustworthy protectors of nucleic acids and improve their bioavailability and internalization into tumor cells in the purpose of tumor suppression [15].

The effects of AuNPs vary with the creative designs of researchers and type of diseases they aim for. In this review, studies with different surface modification of AuNPs, conjunctive methods and therapeutic applications in quantitation and delivery of nucleic acids have been introduced. The graphical abstract of the research of AuNPs is shown in Fig. 1. Their upcoming challenges and future perspectives are also summarized as we hope scientists will be inspired with more futuristic ideas for use of AuNPs in gene theranostics.

2. Application of AuNPs in quantitation of nucleic acids

The biosensing techniques developed with AuNPs mainly depend on their prominent optical properties. As modified with different substances on their surfaces, they are enriched with more possibilities in detecting various kinds of nucleic acids and are empowered with the capability to achieve a much lower detection limit. DNAs, RNAs and other disease-related genes can all be quantitatively detected with functional AuNPs. To provide high sensitivity and selectivity for quantitation of nucleic acids, electrochemical and optical approaches using AuNPs with/without applying nucleic acid amplification (NAA) strategies have been demonstrated. For quantitation of low levels of nucleic acids in the presence of complicated biological matrices, AuNPs-NAA strategies are commonly applied. Some interesting AuNPs-NAA strategies for quantitation of nucleic acids are summarized in Table 1. Target nucleic acids were first amplified with NAA strategies such as RCA, LAMP and DNA walker.

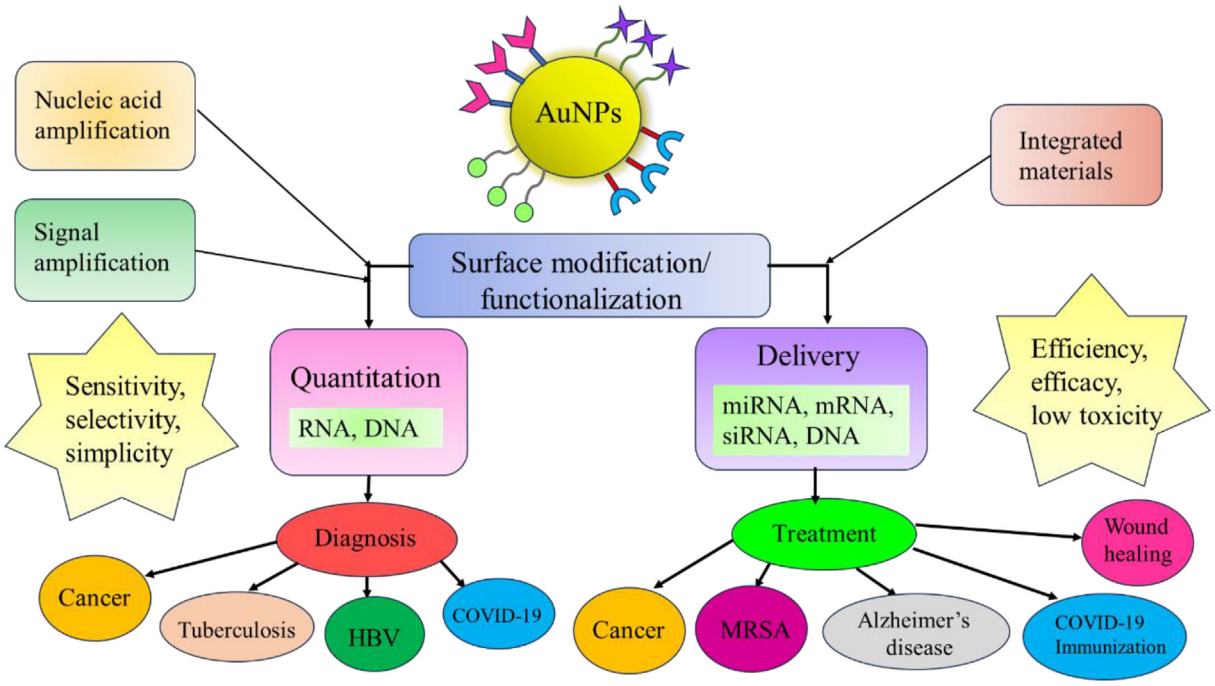

Fig. 1. Summaries of the researches of AuNPs applied in quantitation and delivery of nucleic acids.

Afterwards, they were detected on a AuNPs-based platform functionalized with different materials, achieving lower detection limit and applications for clinical diagnostics. The features and mechanisms of various AuNPs-assisted sensing platforms for nucleic acids are discussed below.

2.1. Analysis of RNA

The miRNA, is one of the well-known biomarkers of cancer and other gene-related diseases. Its abnormality in gene expression may be the indicator of potential tumor growth and disease progression. Thus, sensitive and selective detection of miRNA is of great importance in comprehension of diseases and making efficient treatment plans. In 2021, an ultrasensitive biosensor for detection of let-7 family of miRNAs based on entropy-driven amplification (EDA) coupled with nicking enzyme-assisted AuNP aggregation was introduced [16]. In this study, the EDA recycling process could be specifically triggered. A dual strand containing nicking endonucleases cleavage region is formed as EDA products open the hairpin probe. Afterwards, the addition of nicking endonuclease allowed the product DNA fragments to induce the aggregation of ssDNA-modified AuNPs. The liberating complementary strands continued onto the next cyclic hybridization to obtain the largest signal output. The colorimetric method with signal amplification strategy displayed a limit of detection (LOD) of 3.1 fM, with a wide linear range from 10 fM to 100 pM. Various concentrations have been spiked in10-fold diluted human serum to investigate its application in real samples. The lowest concentration added was 10 fM, with a recovery rate of 99.2%, which also showed promising results. The color change induced by10 fM miRNA in biological samples could be observed by naked eye, showing its potential application in clinical diagnosis. Nicking endonuclease-driven amplification with an electrochemical approach was employed in another study for the detection of miRNA related to cancerous diseases using 3D DNA nanostructures in 2023 [17]. The three-way conjunction structures on the surface of AuNPs were first assisted by target miRNAs. Single-stranded DNAs labeled with electrochemical species were released after nicking-endonuclease cleavage. Via triplex assembly, facile immobilization of ssDNAs could be achieved through pH induced dissociation of the irregular triangular prism DNA (iTPDNA) nanostructure. Level of the target miRNAs was therefore determined by evaluation of electrochemical response, with a linear range from 100 aM to 200 fM and LOD of 10^{-16} M. Different amount of miRNAs were also spiked in two independent serum samples. The SWV responses obtained with high selectivity were quite consistent with those acquired in PBS solution. Catalytic hairpin assembly (CHA) has also been reported to

Table 1. Various AuNPs-based gene analysis integrated with nucleic acid amplification (NAA) methods.

Target nucleic acid	Material for surface modification	Integrated amplification method	Detection limit	Application	Ref.
miRNA	ssDNA	Entropy-driven amplification (EDA) coupled with nicking enzyme	3.13 fM	Cancer diagnosis	[16]
	Irregular triangular prism DNA (iTPDNA)	Nicking Endonuclease-Mediated Amplification (NEMA)	10^{-16} M	Cancer diagnosis	[17]
microRNA-150	Streptavidin	Catalytic hairpin assembly (CHA)	58.90 fM	Diagnosis of incipient diabetic nephropathy	[18]
miR-133b and miR-135b	Carbon dot and DNAzyme strands	DNAzyme Walker	10 fM	Diagnosis of bladder cancer	[22]
miRNA-21	ZIF-8	DNA walker	29 pM	Cancer diagnosis	[19]
	Graphdiyne	DNAzyme walker	0.015 fM	Cancer diagnosis	[20]
	DNA	3D DNA walking	23 pM	Cancer diagnosis	[21]
RNA	Core spherical nucleic acids	PCR	Positive results with dilution factor of 10^5	SARS-CoV-2 diagnosis	[10]
	DNA	PCR	50 RNA copies	SARS-CoV-2 diagnosis	[11]
DNA	not mentioned	Loop-mediated isothermal amplification (LAMP)	42 fg/μLand 103 CFU mL	Testing of COVID-19 and *Enterococcus faecium*	[28]
	Glutathione	Loop-mediated isothermal amplification (LAMP)	100 copies/μL	Point-of-care diagnosis	[29]
	DNA	Rolling-Circle Amplification (RCA)	10 fM	Diagnosis of tuberculosis	[26]
	DNA	Rolling-Circle Amplification (RCA)	5.1 fmol/L	Diagnosis of HBV	[27]
	not mentioned	PCR	340 fmol	Diagnosis of tuberculosis	[25]
Circulating cell-free DNA	HCR hairpin H1	Hybridization chain reaction (HCR)	14.0 pM	Diagnosis of various diseases	[30]

benefit AuNPs-based miRNA detection. Since DNA tetrahedral probe has been found to efficiently capture AuNPs, a ratiometric biosensor for exosomal miRNA detection was developed by integration of tetrahedral probe and CHA [18]. Exosomal miRNA was able to activate the formation of stable duplexes from two hairpin probes in the CHA system. Hybridization of duplexes with barcoded tetrahedra and binding to streptavidin-modified AuNPs (SA-AuNPs) led to a red line visually detected on the test line due to immobilization of SA-AuNPs. The remaining SA-AuNPs captured by biotinylated tetrahedron resulted in a relatively weaker signal compared with that of barcoded tetrahedra. Thus, a ratiometric result was formed as shown in Fig. 2. The linear relationship of this study ranged from 0.1 pM to 10 nM and the LOD was calculated to be 58.90 fM. High sensitivity, selectivity and rapid detection of microRNA-150–5p provided by this assay shows its potential in diagnosis of incipient diabetic nephropathy.

3D DNA walker is also a popular NAA method and has been coupled with AuNPs in quantitation of nucleic acids. A label-free electrochemical sensing platform using 3D DNA walker was designed with metal-organic frameworks (MOFs)-based nanoreactors [19]. Construction of the MOF-based nanoreactors was through encapsulation of GOx in zeolitic imidazolate framework-8 (ZIF-8). The surface of ZIF-8 was loaded with AuNPs by electrostatic absorption. AuNPs were used for anchoring the orbit of 3D DNA walker and promoting electron transfer on electrode interface, which increase sensitivity and promote specificity. The presence of miRNA-21 activated the initiation of 3D DNA walker. Recycling of targets occurred and considerable amounts of fuel DNAs with G-quadruplex/hemin complex on the nanoreactors were immobilized. Subsequently, a cascade catalysis was fulfilled in the limited space of ZIF-8 nanoreactors. Differential pulse voltammetry (DPV) signal was eventually obtained from oxidation of ABTS by H_2O_2, providing a dynamic working range between 0.1 nM and 10 μM, with LOD of 29 pM. Serum samples were also diluted 100-fold for detection. The lowest concentration added was 1 nM. 92%–108% of recoveries were obtained, with RSD values lower than 5.3%, indicating great reproducibility in real sample analysis. The distinguished outcomes and high sensitivity of this proposed method demonstrated a

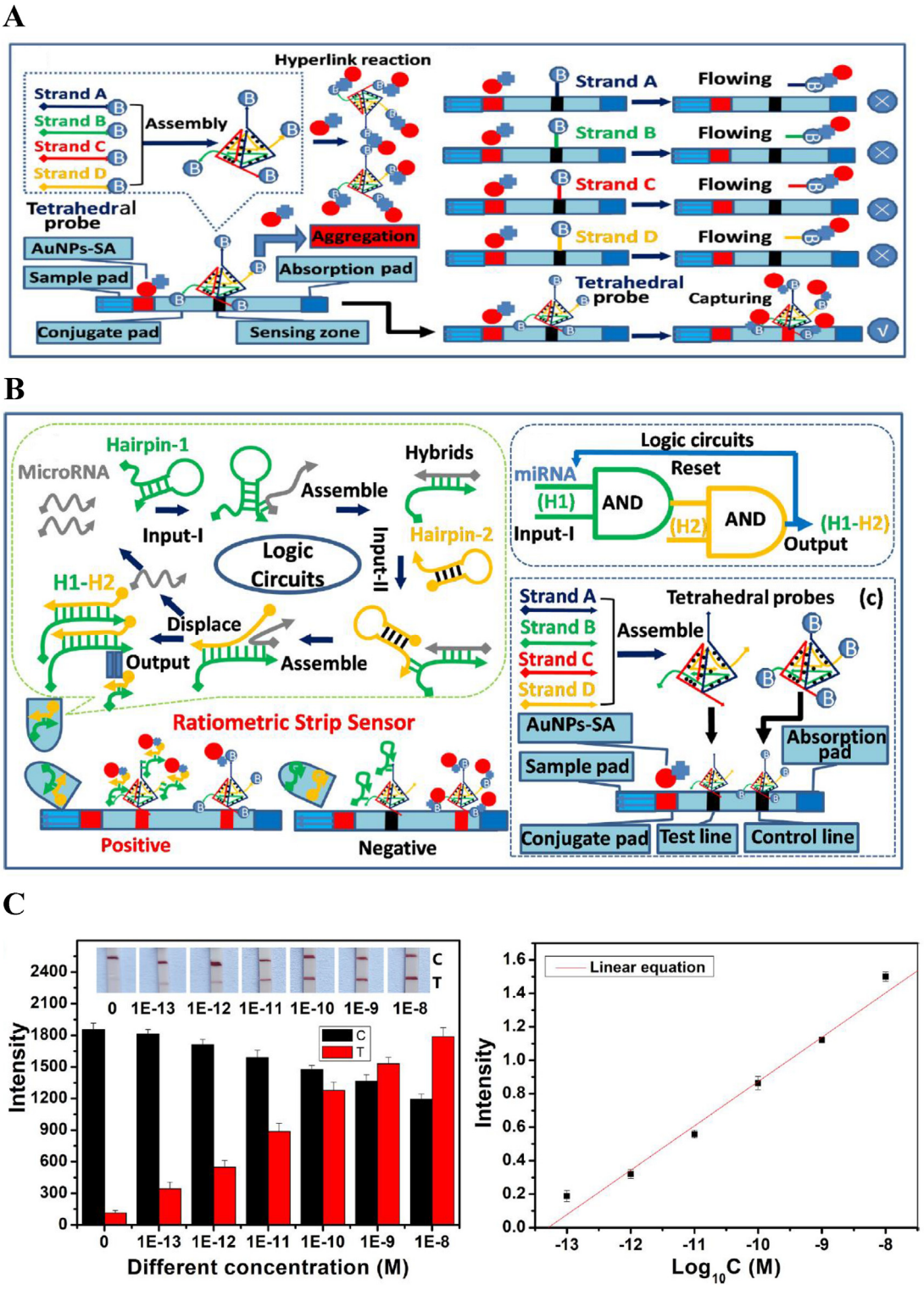

Fig. 2. (A) Design of the tetrahedral capture probes-based lateral flow test strip. (B) Schematic illustration of the ratiometric strip sensor for detecting exosomal microRNA-150–5p. (C) Investigation of the sensitivity of biosensor [18].

novel way to determine miRNA-21 for cancer diagnosis.

A biosensor integrating DNAzyme walker and AuNPs/graphdiyne biosensing interface was developed for quantitation of miRNA-21 [20]. The DNAzyme reaction was first triggered by recognition of miRNA-21, causing considerable glucose oxidase (GOD)-H1 probes cleaved from DNAzyme

walker and hybridized onto the bioanode surface. The substrate reaction was catalyzed by two biocatalysts, glucose oxidase (GOD) and bilirubin oxidase (BOD). The glucose oxidation created a current that was transferred to the biocathode, causing reduction of oxygen, which eventually resulted in open circuit voltage signal. Since AuNPs were modified with graphdiyne, it served as a conductive substrate to accelerate the electron transport speed. As a result, this assay provided a linear range from 0.05 fM to 10 pM, with LOD of 0.015 fM. Spiked experiments to human serum samples were also carried out to evaluate its applicability. The lowest concentration of added miRNA-21 that could be detected was 0.05 fM, with recoveries between 94.40 and 105.7%, demonstrating potential application in real samples. By taking advantage of gene amplification and membrane penetrability of nanomaterials, AuNP-based 3D DNA walking nanomachine was demonstrated for quantitation of miRNA-21, with LOD of 23 pM [21]. The DNA dendrimer was decorated with a substrate strand serving as the DNA track and a DNAzyme restrained by a locking strand as the walker. As DNA dendrimer was employed as a track for intracellular imaging, the nanomachine showcased high directionality and controllability. Precisely regulated distribution of the substrate strand and DNAzyme on the DNA dendrimer could be achieved based on Watson–Crick base pairing, which exhibits superb specificity and predictability. This dendrimer-based nanomachine also displayed stability and anti-interference ability, showing its potential for intracellular cancer cell imaging and monitoring of cancer development. Combination of AuNPs and DNAzyme walker has also been employed for none-invasive and more specific diagnosis of bladder cancer by accurate detection of miRNAs [22]. AuNPs modified with carbon dot (CD)-labeled substrates and DNAzyme strands comprised this novel biosensor. DNAzyme was triggered by target miRNAs, cleaving CD-labeled substrates. The fluorescence intensity recovered as the DNAzyme walked along the AuNPs. Based on the unique design of nanostructure and functionalization of AuNPs, high sensitivity and selectivity was demonstrated, with LOD of 10 fM and a linear range from 50 fM to 10 nM. In clinical specimen, the concentration that could be detected was at picomolar level, which was relatively higher compared with that obtained under experimental conditions. Nevertheless, this method showed good consistency in real samples. Most importantly, exosomal miR-133b and miR-135b in clinical serum samples were simultaneously determined based on multicolor CDs, displaying the potential of the assay for diagnosis of bladder cancer.

Without the assistance of NAA, miRNAs were detected by using luminescent metal organic framework (LMOF) combined with fluorophore-labeled aptamers [23]. The LMOF consisted of ZIF-8 encapsulated with gold nanoclusters possessed unique fluorescence properties. The ligands of the ZIF-8 enhanced the fluorescence intensity of AuNCs while the AuNCs on the surface of LMOF contributed to the fluorescence quenching ability toward fluorophore-labeled aptamers. In miRNA detection, the hybridization of target miRNAs with aptamers caused fluorescence recovery of labeled fluorophores. A linear relationship for miR-21 with a concentration range from 5 pM to 100 pM was obtained. Serum samples of breast cancer bearing mice have also been used for analysis. It has been found that in physical environment, similar linear relationship can be acquired with fluorescence intensity slightly lower than that in PBS buffer. Successful detection of biomarkers of breast cancer (miR-21 and miR-155) corroborated that this biosensing platform is efficient for miRNA sensing. A fluorescent method considering both the advantage of fluorescence imaging and mass spectrometry (MS) was proposed for quantitation of miRNAs [24]. The sensing platform was designed based on fluorophore/mass dual-encoded nanoprobes (FMNPs). Fluorescence imaging could first be achieved by target-triggered hairpin self-assembly and subsequent quantification of miRNAs by MS was later completed. The FMNPs were constructed by AuNPs with decoration of locked hairpin DNA probes (LH1) and corresponding mass tags (MTs) for initial fluorescent detection and consecutive MS readout. miRNA-21 and miRNA-141 activated recycled hairpin self-assembly, causing fluorophore-labeled bolt DNAs to be liberated for production of fluorescent signal. The fluorescence data of miRNAs was then confirmed by MS through reading the ion signal of the barcoded MTs, with linearity between 50 pM and 25 nM and the LODs of miRNA-21 and miRNA-141 of 72 pM and 4.8 pM, respectively. This assay so called “sense-and-validate” strategy served as a model for highly accurate intracellular miRNA quantification and may disclose other genetic events involved in cellular processes of disease development.

2.2. Analysis of DNA

DNA has been validated to be closely related to genetic disorders and gene-related diseases. A variety of NAA methods, including PCR, rolling circle amplification (RCA), hybridization chain reaction

(HCR) and loop-mediated isothermal amplification (LAMP) have been used in conjunction with AuNPs to construct sensitive and efficient sensing platforms for quantitation of low levels of DNA. A sensitive colorimetric assay for detection of tuberculosis DNA based on AuNPs was developed, with LOD of 340 fmol [25]. The DNAs were first amplified by PCR and the plasmonic AuNPs were used as a colorimetric agent with ethanol enhancing its aggregation. Fast response with explicitness was achieved within 3 min after addition of DNA amplicons. The color of AuNPs changed from red to purple as the solution contained PCR products from tuberculosis DNA. Since real clinical samples contain limited amount of TB DNA, artificial sputum has been prepared to estimate its applicability. 2 ng/μL spiked DNA validated that this strategy may also be feasible in clinical application. Simplicity and robustness of this sensing platform may bring more prospects for employment as tuberculosis screening tool, especially in places short of high-accuracy sensing equipment. RCA implemented with AuNPs was demonstrated for tuberculosis DNA detection, with LOD of 10 fM [26]. Through RCA, a large number of oligonucleotides were produced from target DNA, followed by hybridization of amplified oligonucleotides with the capture DNA of AuNPs and magnetic beads, in the form of a sandwich structure. The sandwich structure was then magnetically separated and AuNPs were dehybridized and released from the magnetic beads. The AuNPs was applied onto the amine-modified coverslip, where they could be functionalized with negative charge and evenly distributed for dark-field image acquisition. Because the template used in this method is universal for diverse targets except for the sequence related to the target, the necessity of changing capture DNA sequences on magnetic beads and AuNPs for different targets is not needed. Furthermore, the possibility of clinical application was verified by spiking various concentrations of DNA into real samples. It was found that the recoveries of 1 pM and 100 pM target were 100% and 86.2%, respectively, demonstrating ideal feasibility. RCA-AuNPs was developed for detection of DNA of hepatitis B virus through single particle inductively coupled plasma mass spectrometry (spICP-MS) [27]. When the target DNA was present, RCA was triggered and large amount of ssDNAs with repeating sequence units were generated. Through complementary base pairing, the DNA-labeled AuNP probes first hybridized with HBV DNA, assembling into long chains and eventually aggregated into large particles. Agglomeration of AuNPs after the addition of RCA products and spermidine resulted in marked pulse signals in spICP-MS. Under optimal conditions, this method exhibited high sensitivity and selectivity, with a linearity of 10–2000 fmol/L and LOD of 5.1 fmol/L. The developed method was also applied to serum samples from healthy human. 0, 40, 100, and 500 fmol/L target HBV DNA was added to perform the recovery test. 94.2–108% of recoveries were obtained, showing great potentiality in actual sample analysis. The schematic illustration of HBV DNA analysis and the experimental results are shown in Fig. 3.

In addition to RCA, LAMP is commonly combined with AuNP in quantitation of nucleic acids. LAMP-AuNPs was successfully demonstrated for point of care testing of Coronavirus (COVID-19) and *Enterococcus faecium* (*E. faecium* spp.) [28]. Target DNAs were first amplified by LAMP, which interacted with gold ions dissolved in the samples. Upon UV illumination for less than 10 min, a red color solution of AuNPs was observed. The LODs of COVID-19 plasmid DNA and *E. faecium* spp. were as low as 42 fg/μL and 10^3 CFU/mL, respectively. The LOD of *E. faecium* spp. was obtained in real samples, revealing that this method can be useful for clinical diagnosis of infectious disease. Interestingly, it has been discovered that AuNPs not only be employed with LAMP but has the ability to enhance LAMP efficiency directly [29]. The effects of GSH-capped AuNPs on various reagents in LAMP reaction such as Mg^{2+}, template DNA, dNTPs, primers, and polymerase were investigated. The addition of AuNPs to primers showed negative influence on LAMP. In contrast, mixing AuNPs with other reagents stimulated the amplification process. The enhancement on LAMP was most notable when AuNPs formed a protein-like surface. Besides, GSH was found to be the most efficient modifying material compared with other ligands such as polymers, inorganic ions and DNAs. Under optimal conditions, the approach allowed detection of target DNA down to 100 copies/μL, with linearity from 1.26×10^7 to 1.26×10^3 copies/μL.

Circulating cell-free DNAs (cfDNA) have been generally analyzed for identification of various ailments. They are DNA fragments released in body fluids, which are considered popular biomarkers for cancer and a variety of illnesses. However, most of the analytical methods reported for cfDNA lacks sensitivity and requires intensive labor. A unique platform coupling hybridization chain reaction (HCR) with AuNPs for detection of cfDNA was developed, with linearity of 25 pM–100 nM and LOD of 14.0 pM [30]. HCR hairpins (H1 and H2) were designed with one-base mismatch to enhance the reaction efficiency, in which H1 molecules were

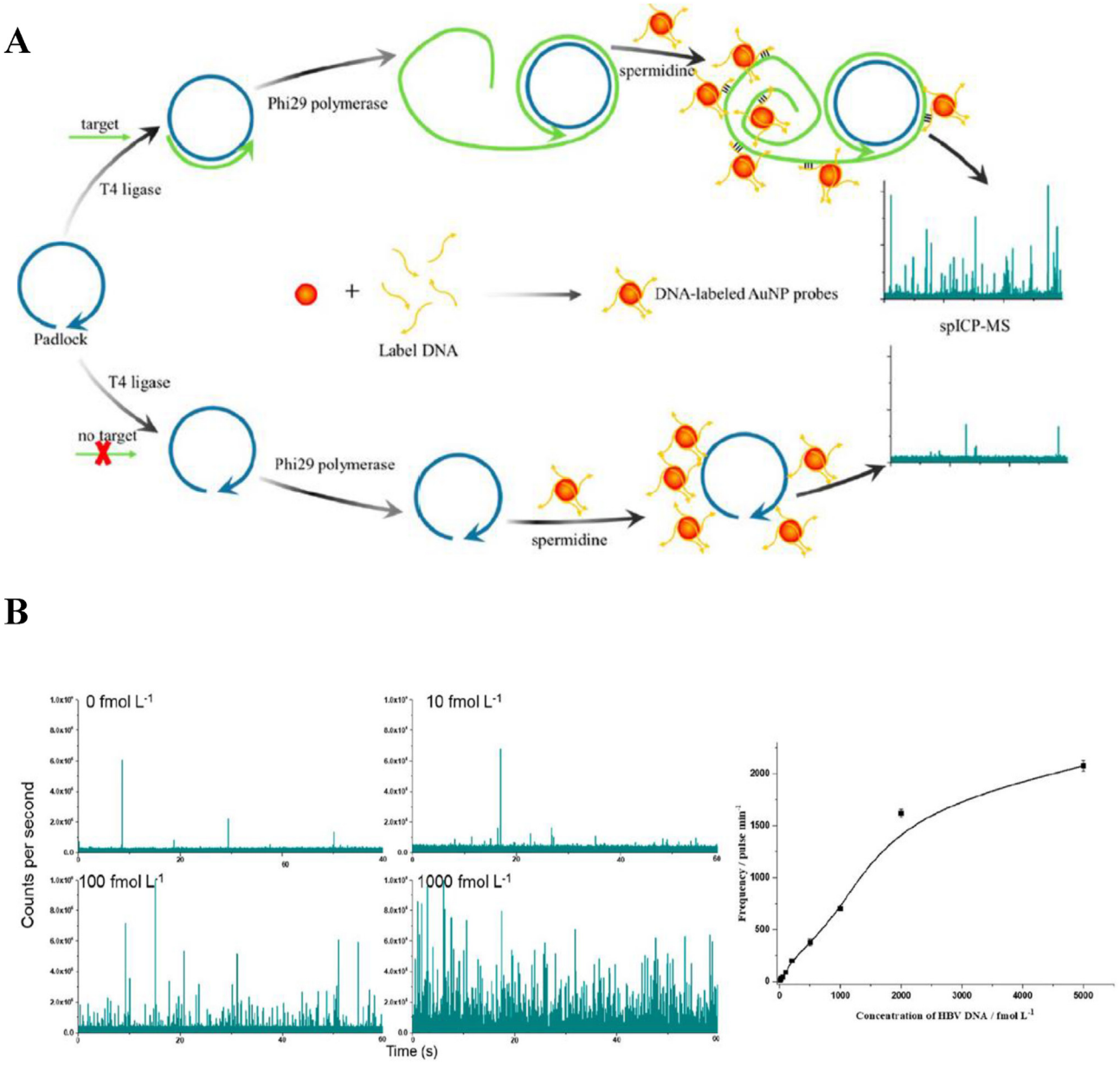

Fig. 3. (A) Schematic illustration of the detection of HBV DNA with RCA and AuNP tags. (B) spICP-MS profile spectra of different target concentrations [27].

bound to the surfaces of AuNPs through polyadenine. Two different domains were designed for target cfDNA. One has the capability to activate HCR for generation of dsDNA concatemer carrying numerous AuNPs; the other was responsible for hybridization with capture DNA on the surface of Ω-shaped fiber optic (FO) probe. The presence of cfDNA initiated the HCR and brought dsDNA concatemer with AuNPs to the probe surface, producing dramatically enhanced localized surface plasmon resonance signal. The performance of the biosensor in clinical application was also evaluated by spiking different concentrations of cfDNA in serum samples. The lowest concentration added was 0.05 nM and the recoveries obtained were within the range of 88.54%–112.80%, indicating good feasibility of detection in actual samples. The schematic illustration of cfDNA analysis and the experimental results are shown in Fig. 4.

Without the assistance of NAA, efficient DNA analysis can also be achieved. A colorimetric method based on DNA-functionalized AuNPs for diagnosis of *Neisseria gonorrhoeae* infection with LOD of 15.0 ng within 30 min was reported [31]. Through complementary annealing, DNA-functionalized AuNPs hybridized with genomic

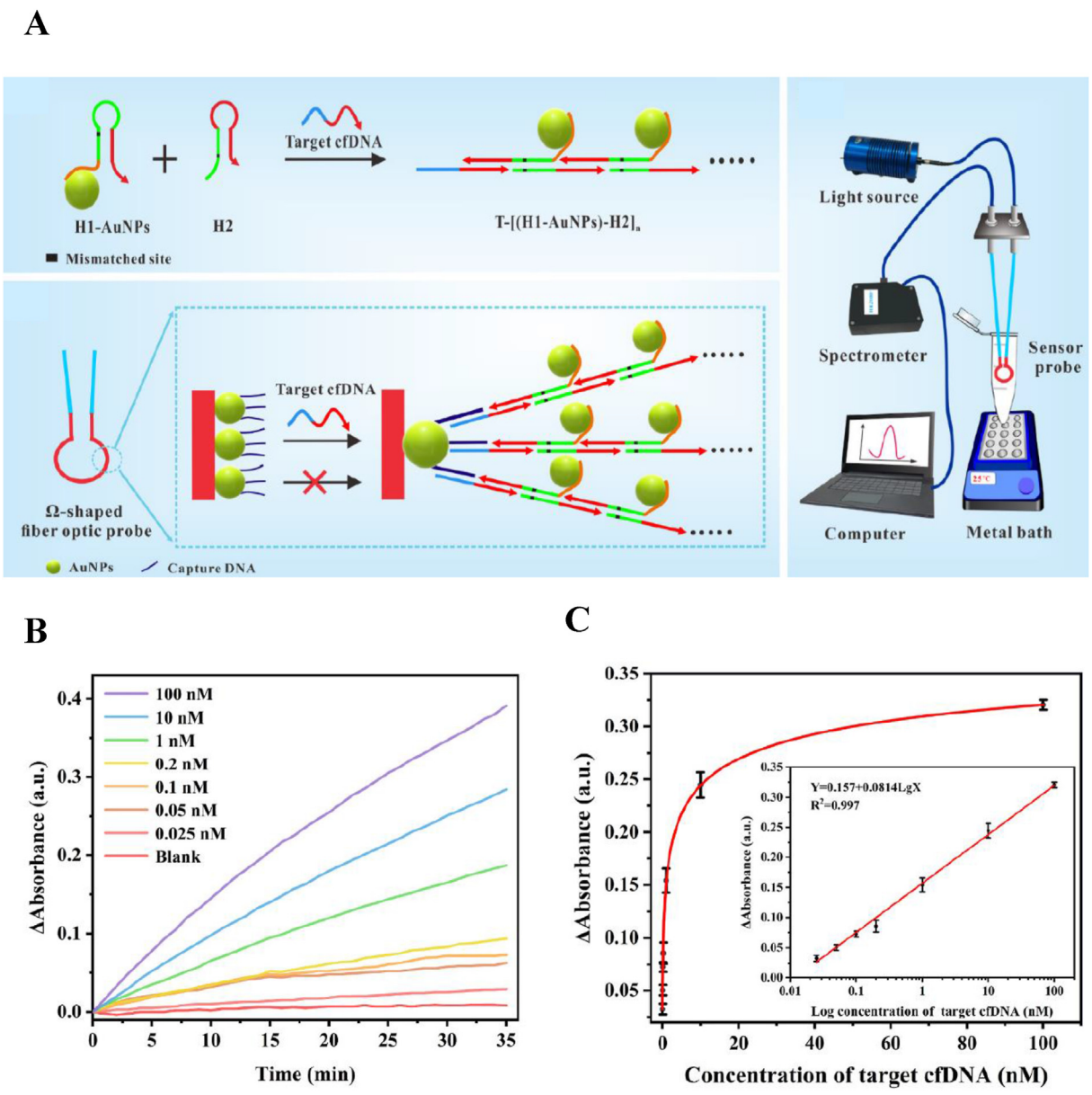

Fig. 4. (A) Schematic diagram of Ω-shaped FO-LSPR biosensor based on mismatched HCR and AuNPs for cfDNA detection. (B) Time monitoring results for detection of target cfDNA with different concentrations. (C) The net change of absorbance with the increased concentration of cfDNA [30].

gonococcal DNA with its ability to target DNA uptake sequence. Afterwards, improvement in salt stability of nanoprobes upon annealing to a reverse complementary oligonucleotide was observed. On the contrary, in high salt media DNA-functionalized AuNPs became unstable, aggregating into larger molecules with a color change from red to blue. AuNPs can act as a signal amplifier in electrochemical sensing of nucleic acid fragments from synthesized branched DNAs, with linearity from 0.10 pM to 10 nM and LOD of 0.09 pM [32]. The DNA probes were synthesized with three different sticky ends. One was assembled on the gold electrode via Au−S bond. The other two were designed to capture target DNA. The sandwich structure formed by DNA probe, target DNA, and DNA-modified AuNPs resulted in an electronic signal since the hybridization process between DNA probe and target DNA changed the surface structure of the electrode and affected the electron transfer rate.

Besides above spherical AuNPs, various shapes of Au nanomaterials have been used for quantitation of DNA. A lateral flow biosensor based on Au nanorods (AuNRs) was developed for detection of DNAs, with linearity from 0.01 to 10 nM and LOD of

2 pM [33]. The DNA probe was labeled with a colored tag designed with AuNRs, while the capture probe was immobilized on the test region of biosensor. When the target DNA was present, the AuNRs tagged detection probe, target DNA and capture probe formed a sandwich structure based on Watson-Crick base pairing. AuNRs seized on the test region accumulated, resulting in a characteristic colored band. To investigate the applicability of this AuNRs-based biosensor, a series of DNA concentrations were spiked into serum samples. The lowest concentration found detectable was 50 pM, with recoveries ranged from 92.0 to 103.1%. An electrochemical biosensor using gold nanostars (AuNSs) was demonstrated for quantitation of Z3276, a genetic biomarker of *Escherichia coli* O157:H7 (*E. coli* O157:H7) [34]. The surface of gold coated electrode was functionalized with AuNSs to increase its surface area and detection sensitivity. Specifically animated DNA probes, labeled with toluidine blue, were immobilized onto the electrode and the active sites were blocked by mercaptoethanol to prevent non-specific adsorption. In the presence of the target DNA, the electrochemical response on the electrode was enhanced, leading to increases in current, which enabled DNA quantification by square wave voltammetry technique. The linear response was in the range of 7.3 to 10^{-17} μM and the LOD in environmental water samples was as low as 0.01 zM, corroborated its potential application in food safety and monitoring of the environment. Surface enhanced Raman spectroscopy (SERS) is also a popular and versatile method for characterization of virus particle that can be enhanced by novel gold nanomaterials. Gold nanocubes (AuNCs) with an average size of 50 nm were employed for signal amplification of SERS in HIV-1 DNA detection [35]. The HIV-1 DNA strands were coated with AuNCs to increase the intensity values. Three new peaks at 421 cm^{-1}, 1069 cm^{-1} and 1254 cm^{-1} were detected in HIV-1 DNA compared with the Human Random Control DNA. A good linear relationship between peak intensity at 1257 cm^{-1} and 1570 cm^{-1} and HIV-1 DNA concentrations ranging from 1 to 20 nM were obtained. Gold bipyramidal nanoparticles (AuNBs) were also used for quantitation of DNA through SERS, with LOD of 10^{-9} M [36]. Through self-assembled AuNBs after binding with DNA, strong Raman signals were detected. Quantitative DNA analysis was achieved with a satisfactory linear relationship between the DNA base intensity and concentration. Moreover, this platform was applied to identify DNAs in methylated DNA, serum, and cell metabolites. Although the characteristic peaks of DNA in serum samples were affected by a variety of complex substances, this platform still serves as an experimental basis for diagnosis of genetic diseases.

Among all the optical detection techniques, colorimetric methods offer fast, simple, affordable and even portable sensing device to scientists since many of the existing techniques are usually time-consuming, complicated and labor-intensive. Besides, it can respond to a wide range of analytes. Nevertheless, the reactions of analytes are determined by naked eye, which may be discrepant from different observers. Colorimetric methods also have difficulties in determining one particular component in a complex mixture. Thus, designing substance-specific sensors with clear color change may overcome limitations of these techniques. There are many advantages when AuNPs are used in conjunction with SERS, including high sensitivity, chemical specificity, non-destructive and label-free analysis. However, it still faces several challenges such as reproducibility, biological recognition and molecular interaction. Reproducibility can be solved by selecting substrates with higher chemical stability. Biological recognition could be improved by modification with various polymers with higher affinity to the analytes. In the aspect of molecular interaction, the number of hot spots and the sites where substrates are conjugated to the molecules are critical to sensitivity. The signal can be dramatically enhanced by locating the analytes at the center of the hot spot instead of outside of it. Fluorescent assays combined with AuNPs are known for its swift response, easy operation and requirement of small sample volume. The problems often found with fluorescent detection are short lifespan of fluorophores and mistaking fluorescent signals of other substances when the analyte concentration is too low. Proper solutions may be promoting the efficiency of nucleic acid amplification to assure that the analytes can be quantitatively determined in limited time. Optimizing the protocol of nanomaterial synthesis may also offer more possibilities of extending the fluorophores' lifespan.

In these reviewed methods, the LODs were totally different. However, the sample matrix were various among these method, and it is difficult to conclude which detection technique would possess the wonderful detection sensitivity. Generally, the LODs achieved by actual samples are usually poorer than those from cells. This is mainly because clinical samples are usually complex and contain diverse interfering factors. During sample preparation, the purity of extracted samples is a major concern before analysis. The stability of the

analytes and amplification reaction may be also affected by the enzymes, reagents and surfactants used for cell lysis. Unnecessary substances and other contaminants may cause serious interference to the signal. To ensure high purity of extraction and minimize undesirable outcomes, it is fundamental to optimize the conditions of sample preparation, including reagent composition, type of elution and washing buffer, stationary phases and elution volume. Adjustment of pH value may facilitate binding and release of analytes, leading to higher sensitivity and selectivity. The use of chaotropic agents also revealed that lysis efficiency can be promoted by using more than one lysis agents simultaneously. Besides, developing more sensitive detection probe conjugated to the surface of AuNPs is also an effective approach to determine target nucleic acids in clinical samples. Storage of nucleic acid sample is also critical. Since nucleic acid samples are usually stored between −20 °C and −80 °C, it is extremely expensive, energy-consuming and requires rigorous management to meet such criteria. In addition, repeated freeze-thawing should be avoided as it may cause sample precipitation, decreasing the sensitivity of analysis. Encapsulating nucleic acids into microcapsules resistant to environmental denaturation may be an alternative to conventional measures. It allows storage at room temperature while preserving its fidelity, lowering the concentration that can be reliably detected.

3. Delivery of nucleic acids

In order to manipulate effective gene therapy, efficient delivery of nucleic acids is a fundamental issue that has been popularly discussed by researchers worldwide. Various nanomaterials such as AuNPs, carbon nanomaterials and liposomes have been considered in the development of gene delivery system. However, utilization of them face different degrees of difficulties in delivery efficiency, cytotoxicity, biocompatibility and cell permeability. Having advantages of ease in preparation and conjugation, brilliant biocompatibility, stability, great cellular uptake and transfection efficiencies, AuNPs have become one of the most important carriers for delivery of nucleic acids. Unique techniques innovated with AuNPs for delivery of nucleic acids are summarized in Table 2. To offer effective treatments for various diseases, AuNPs-based nanovectors are functionalized with a diversity of organic and inorganic molecules, targeting different genes. Their characteristics and process of gene delivery are explained as follows.

3.1. Delivery of RNA

3.1.1. miRNA

miRNAs are not only widely-used biomarkers of cancer but also contribute significantly to either proliferation or suppression of tumor cells. Thus, regulating miRNA expression emerges new possibilities for management of cancerous diseases. To deliver miRNA-206 to tumors of Luminal A type breast cancer, PEGylated AuNPs were prepared [37]. The AuNPs carrying miRNA-206 arrest cells in the G0-G1 phase, causing cell deaths in MCF-7. Moreover, cell apoptosis was triggered after down-regulation of NOTCH 3. Great efficiency shows the potential of PEGylated AuNPs to deliver miRNA for cancer treatment.

AuNPs were used for successful delivery of miR-21-3p for melanoma treatment, with evidence of increased ferroptosis sensitivity [38]. IFN-γ-mediated ferroptosis was facilitated since miR-21-3p targeted thioredoxin reductase 1 (TXNRD1) directly, leading to enhancement of lipid reactive oxygen species (ROS) generation. Besides, transcription of miR-21-3p in IFN-γ-mediated ferroptosis could be promoted by ATF3 that is a transcription factor playing a pivotal role in oncogenesis. In addition, anti-PD-1 antibody was synergized with miR-21-3p overexpression to further control tumor cells. In the systemic delivery experiment of the mice model, 10 mg/kg of miR-21-3p administered intraperitoneally to each mouse. This high delivery efficacy without apparent side effects shows the immunotherapy potential of this approach for cancer patients. Delivery of miRNA is not only limited to one single gene or agent. Co-delivery of dexamethasone and a microRNA-155 inhibitor (miR-155i) was reported with a nanoplatform constructed with generation 5 (G5) poly(amidoamine) dendrimer entrapped AuNPs (Au DENPs) [39]. The Au DENPs were designed to provide a combination therapy consisting of steroids and gene for effective treatment of acute lung injury (ALI). With ideal cytocompatibility, the Au DENPs allowed efficient delivery of dexamethasone and miR-155i. In the animal experiment, 0.25 mg/kg of miR-155i was injected intraperitoneally. As miR-155i reached lipopolysaccharide (LPS)-activated alveolar macrophages, the suppressor of cytokine signaling 1 and IL-10 expression were both upregulated simultaneously, while proinflammatory cytokines, including TNF-α, IL-1β, and IL-6, were downregulated. Meanwhile, cyclooxygenase-2 expression in the LPS-activated alveolar macrophages was downregulated by dexamethasone, leading to inhibition of pro-inflammatory cytokine secretion. The

Table 2. Various methods for gene delivery by using AuNPs.

Type of gold nanoparticles	Material for surface modification	Type of nucleic acid delivered	Delivery target	Application	Ref.
AuNPs	G5 poly(amidoamine) dendrimer	microRNA-155 inhibitor	Lipopolysaccharide (LPS)-activated alveolar macrophages	Therapy for acute lung injury	[39]
	PEG moiety	microRNA-206	MCF-7 cell	Breast cancer treatment	[37]
	not mentioned	miR-21-3p	Thioredoxin reductase 1 (TXNRD1)	Melanoma treatment	[38]
	Dendrimer (PAMAM G5D)	mRNA	Folate receptor	Gene therapy	[41]
	11-amino-1-undecanethiol acid (AUT), polyethyleneimine (PEI) molecules	mRNA	HEK293 cell	Gene therapy	[42]
	PEG, cell-penetrating peptide	Oligonucleotide	Telomerase RNA template subunit	Cancer treatment	[59]
	Polyethylenimine	Oligonucleotides	mecA gene	MRSA treatment	[58]
	PF127 gel	siRNA	Prostaglandin transporter (PGT) gene	Diabetic wound healing	[54]
	Diblock copolymer	siRNA	C9orf72	Treatment for amyotrophic lateral sclerosis	[52]
	Tat-related cell-penetrating peptide	siRNA	Secreted embryonic alkaline phosphatase (SEAP)	Retinal pigment epithelial cell drug delivery	[53]
	Collagen	siRNA	EGFR receptor	Lung cancer treatment	[45]
	Dendrigraft Poly-L-Lysine (d-PLL)	siRNA	PC-3 PSMA cell	Prostate cancer treatment	[47]
	Chitosan	siRNA	H1299-Egfp	Lung cancer treatment	[46]
	Polyethyleneglycol (PEG)	siRNA	APOE4	Treatment for Alzheimer's disease	[51]
	Y-shaped DNA bricks	siRNA	Plk1 mRNA and PLK1 protein	Cancer treatment	[43]
	Carbosilane dendrons	siRNA	HL-60 and CEM-SS cell	Cancer treatment	[44]
Gold nanocages	Lactoferrin, diaminobutyric polypropylenimine dendrimer	DNA	TNFα	Prostate cancer treatment	[57]
Gold nanorods	Dendrimer (PAMAM, G3)	gene FAM172A	HCT-8 cell	Colon cancer treatment	[60]
	Polyethyleneimine, RGD (arginine-glycine-aspartic acid).	MicroRNA-320a-3p	Sp1	Lung cancer treatment	[40]
	Peptides	siRNA	Notch1	Management of breast cancer metastasis	[49]
	Cell-penetrating peptides	siRNA	Transcription factor EB	Osteosarcoma treatment	[50]
Gold nanostar	Chitosan	DNA	S protein	Immunization of COVID-19	[56]
	Cationic tumor-targeting peptide, PEG	siRNA	Panc02	Anticancer therapy	[48]
	not mentioned	siRNA, mRNA	ARPE-19 cell	Retinal pigment epithelial cell drug delivery	[55]

expected regulation of target genes helped repair the damage lung tissues and may be hopefully applied in other anti-inflammatory therapies. The schematic illustration of dexamethasone and miR-155i co-delivery and the experimental results are shown in Fig. 5.

Successful delivery of miR-320a was reported with polyethyleneimine and arginine-glycine-aspartic

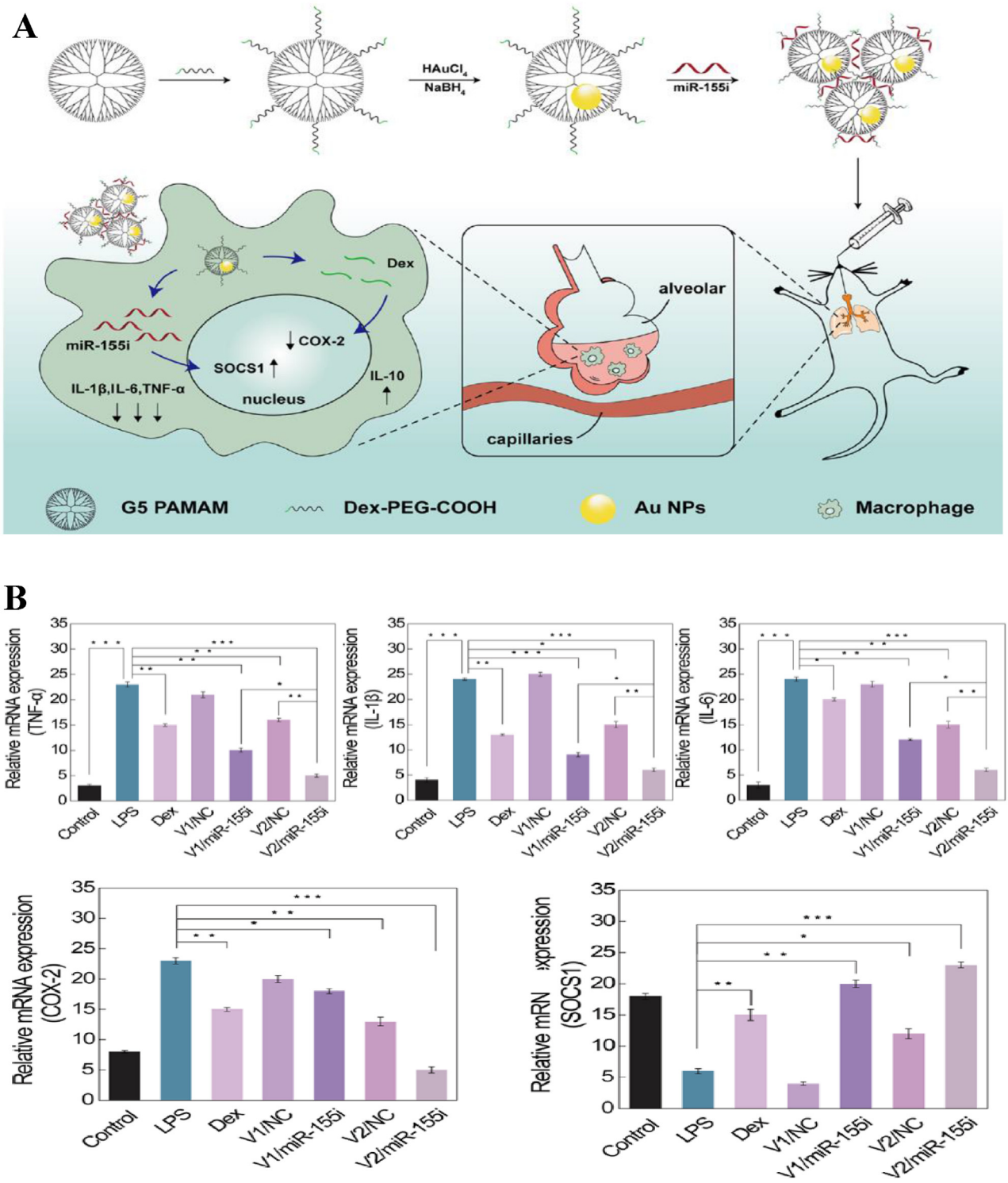

Fig. 5. (A) Preparation of nanocomplex for combined anti-inflammatory chemo-gene therapy of ALI. (B) RT-PCR assay of the mRNA expression of different inflammation-related factors [39].

acid (RGD)-modified AuNRs for lung cancer therapy [40]. With the ability to bind to integrin αvβ3 specifically, RGD ligands enabled miR-320a to be carried to lung cancer cells, targeting Sp1. 10 μg/mL of miR-320a was chosen as the transfection concentration. As miR-320a reached the cancer cells, direct binding to the 3′UTR of Sp1 suppressed its expression, which led to final enhancement for

expression of phosphatase and tensin homolog and downregulation of matrix metallopeptidase 9, augmenting apoptosis and DNA damage. Under laser irradiation, the release of miR-320a increased and the inhibition of the proliferation and metastasis of cancer cells by miR-320a enhanced. No obvious toxicity to A549 cells and high efficiency allowed the delivery system to be implemented in a wide variety of gene delivery.

3.1.2. mRNA

mRNAs, responsible for carrying instructions from DNA and creating proteins in cells have also inspired scientists' interests in therapeutic applications. Efficient delivery of luciferase reporter gene (FLuc-mRNA) was evaluated with formulation of folic-acid-(FA)-modified, poly-amidoamine-generation-5 (PAMAM G5D)-grafted AuNPs [41]. Nanocomplexes contained 0.05 μg mRNA with varying amounts of nanoparticles were prepared for evaluation of delivering efficiency. The compaction of the targeted nanocomplexes contributed to weak binding of mRNA, which helps with dissociation of mRNA from nanocomplex and avoidance of degradation by the lysosomal compartment. As expected, the nanocarrier provides advantages of against nucleases digestion of mRNA from RNAase A and significantly higher ($p < 0.0001$) transgene expression in folate receptors of MCF-7 and KB cells. The folate-receptor-mediated delivery was further proved to be the major route for the nanocarrier to enter receptor-positive cells, with a support of much lower transfection levels in the FA receptor negative cell lines than that of the positive ones. Improvement in mRNA delivery with respects to efficiency of cytoplasmic delivery and transfection capacity was demonstrated using AuNPs functionalized with two different cationic molecules, 11-amino-1-undecanethiol acid (AUT), polyethyleneimine (PEI) [42]. Through the statistical analysis of the GFP expression quantification, significant increase in fluorescence signal was achieved using the PEI-AuNPs. The highest ratio of mRNA to AuNPs reached 5000, indicating high loading capacity. Efficient cytoplasmic release of mRNA was achieved by "proton sponge" effect. The risk of nucleic acid degradation was reduced and the surface saturation was ensured by performing the incubation at 4 °C for 24 h. Even though the transfection efficiency of 50 nm PEI-AuNPs was not great, the GFP expression was able to sustain for seven days with limited cellular damage. Besides, promotion of protein expression was obtained when the transfection was operated with chloroquine.

3.1.3. siRNA

Small interfering RNAs (siRNAs) are regulators of the expression of multiple mRNAs. They bind to complementary sequences of mRNA in the purpose of short-term switching off of particular genes. The delivery of siRNA has been concerned for effective gene-mediated therapy for numerous illnesses. AuNPs tiled with anti-degradation Y-shaped backbone-rigidified triangular DNA bricks with sticky ends (sticky-YTDBs) were employed for efficient and stable siRNA delivery [43]. A multi-functional three-dimensional (3D) DNA shell was formed after tiling DNA bricks on the surface of each AuNP and a biocompatible nanovector was constructed after arrangement of aptamers on its exterior surface. An equal amount (10 μL, 10 μM) of sense strand and antisense strand were mixed for the preparation of siRNA loading. SiRNAs encapsulated in the interior 3D DNA shell were protected by the YTDB on the outer layer against enzymatic digestion from endogenous nucleases. The release of siRNAs was realized as ADCs (anchoring DNA complementary to miRNA) preferentially hybridized with endogenous miRNA-21. As siRNAs reached their targets, the expression of Plk1 mRNA and PLK1 protein was silenced, inducing apoptosis. With advantages of against enzymatic degradation and nonspecific cell permeation, the nanovector possessed longer blood circulation lifetime which provided siRNA with adequate time to reach tumor tissues and escape from the endosome into cytoplasm, resulting in enhanced gene silencing capability of siRNA.

AuNPs modified with cationic carbosilane dendrons of 1–3 generations (AuNP13, AuNP14, AuNP15) could bind siRNA effectively [44]. AuNP14 and AuNP15, with higher molecular weight and number of molecules, were shown to be more toxic, but with lower concentration required for delivery and higher cellular uptake, likely because of their greater flexibility to adjust their shape and tightly bound to siRNAs. The concentration used for siRNA delivery was 100 nM. Cellular uptake with AuNP15 reached 50–60% for HL-60 and CEM-SS cells after 3 h before decreases due to degradation of the complexes in lysosomes. The release of siRNA took about a day as some biophysical conditions may be interfering. Cell death was analyzed after 48 h by inhibiting proteins of the bcl2 family, showing that the dendronized AuNPs activated cell deaths independently. AuNPs modified with biocompatible materials such as proteins and liposaccharides have been shown promised for siRNA delivery. AuNPs conjugated with collagen for delivery of EGFR siRNA were demonstrated for treating lung cancer [45]. The siRNA s were loaded by interaction of

AuNPs with EGFR siRNA at 3:2 volume ratio. Higher efficiency in carrying siRNA to silence EGFR gene expression of A549 cells was achieved in comparison with lipofetamine. Release of siRNA was realized by disassociation with positively charged amine groups of collagen. Nuclease degradation of siRNA was successfully prevented by AuNPs. The cell entry was mediated by endocytosis and the AuNPs were later metabolized by lysosomes. In xenograft mice model, effective tumor growth suppression was observed with 70% reduction in tumor weight, whilst only a 30% decrease was carried out with lipofetamine. Chitosan (CS)-coated AuNPs prepared according to a layer by layer (LBL) self-assembly method were employed to enhance siRNA delivery [46]. Positively charged CS-AuNPs were first modified with a layer of siRNA cargo molecules, followed by another layer of chitosan to protect siRNAs from fast release and to provide positive charges for strong interaction with cells. SiRNA loading capacity was evaluated by mixing siRNA and CS-AuNPs at different mass ratios, ranging from 1:0.5 to 1:12.5. The results showed that 1:7.5 reached full loading. The layer-by-layer design offered advantages of colloidal stability and controlled siRNA release. Downregulation of enhanced Green Fluorescent Protein (eGFP) in H1299-eGFP lung epithelial cells provided supportive evidence for protection of siRNA against enzymatic degradation in the LBL-CS-AuNPs. Improved cellular uptake by endocytosis and endosomal escape of siRNA were also manifested. The schematic illustration of siRNA delivery and the experimental results are shown in Fig. 6. AuNPs coated with Dendrigraft Poly-L-Lysine (d-PLL) were fabricated to deliver siRNA targeting folate receptors efficiently [47]. Tetrachloroauric acid were reduced by ascorbic acid after the addition of d-PLL, forming a positively charged nanocomplex with high stability in aqueous solution. The loading capacity was found when the mass ratio of AuNPs over siRNA was 30. The AuNPs-d-PLL was further modified with folate-targeted Poly(ethylene glycol) in order to bind to the folate receptor of PC3-PSMA cells more specifically while shielding naked siRNAs from enzymatic degradation. The release of siRNA was achieved by ruptures of vesicles caused by osmotic swelling. Cellular uptake of the nanocomplexes by prostate cancer cells were evaluated by flow cytometry and Laser Scanning Microscopy imaging.

Alternatively, high-surface gold nanostars (AuNS−P) decorated with cationic tumor-targeting peptide functioned as a nanocarrier of siRNA were employed to deal with cancer [48]. Large amounts of siRNA (0.1 μg) were loaded on the nanoplatform thanks to the positively charged amino acid sequence and large surface area. Moreover, with the help of amino acids and RGD sequence, AuNS−P was able to identify integrin receptors on the tumor cell membrane and get internalized through its phospholipid bilayer. The siRNAs were released by the platform and acted on the target mRNA thanks to the proton sponge effect of the arginine-rich peptide in the acidic lysosomal environment. Additionally, prolonged circulation time and functionalization of targeting peptide was demonstrated by modification of PEG AuNS−P's surface, which led to noticeable tumor accumulation.

Multivalent peptide-functionalized AuNRs with high stability against protease and specific targeting cMET receptor were found to efficiently carry siRNAs for treatment of breast cancer [49]. In this study, the peptide/siRNA molar ratio was maintained at 50:1 and the siRNA concentration was taken as 25 nM. Successful endosomal release of siRNA was validated by estimation of nanocomplex-mediated rupture using giant unilamellar vesicles. Phagocytosis and degradation by the macrophages were effectively prevented. The functional AuNRs with low cytotoxicity allowed efficient silencing of Notch1 gene that plays a pivotal role in cell proliferation and inhibition of metastasis in triple-negative breast cancer cells (MDA-MB-231). Anti-metastasis in cells with silenced Notch1 gene was witnessed with restraining the progression of epithelial-mesenchymal transition (EMT). To avoid relapse of osteosarcoma generated by cytotoxicity, failed targeting and resistance to photothermal-induced autophagy, AuNRs functionalized with cell penetrating peptides (CPP) were synthesized for siRNA delivery [50]. The siRNAs bound almost completely to AuNRs when the mass ratio of AuNRs to siRNA was 16:1. The pH-sensitive CPPs increased the uptake efficiency of the CPPs functional AuNRs by osteosarcoma cells and precision of tumor targeting. Besides, the CPP-conjugated AuNRs minimized unwanted degradation and released siRNA at a steady rate by inhibiting formation of autolysosomes and eliminating resistance of autophagy to photothermal therapy. Under NIR irradiation, cancer cell ablation and anti-metastasis induced by the CPP-conjugated AuNRs were further enhanced.

In addition to cancer, significant progress has been made in AuNPs-assisted siRNA delivery for treatments of other diseases. The studies were conducted with 1 μM of siRNA. Two different forms of pegylated AuNPs (PEG-AuNP14a and PEG-AuNP14b) were capable of crossing blood brain barriers and carrying siRNAs targeting APOE4 for

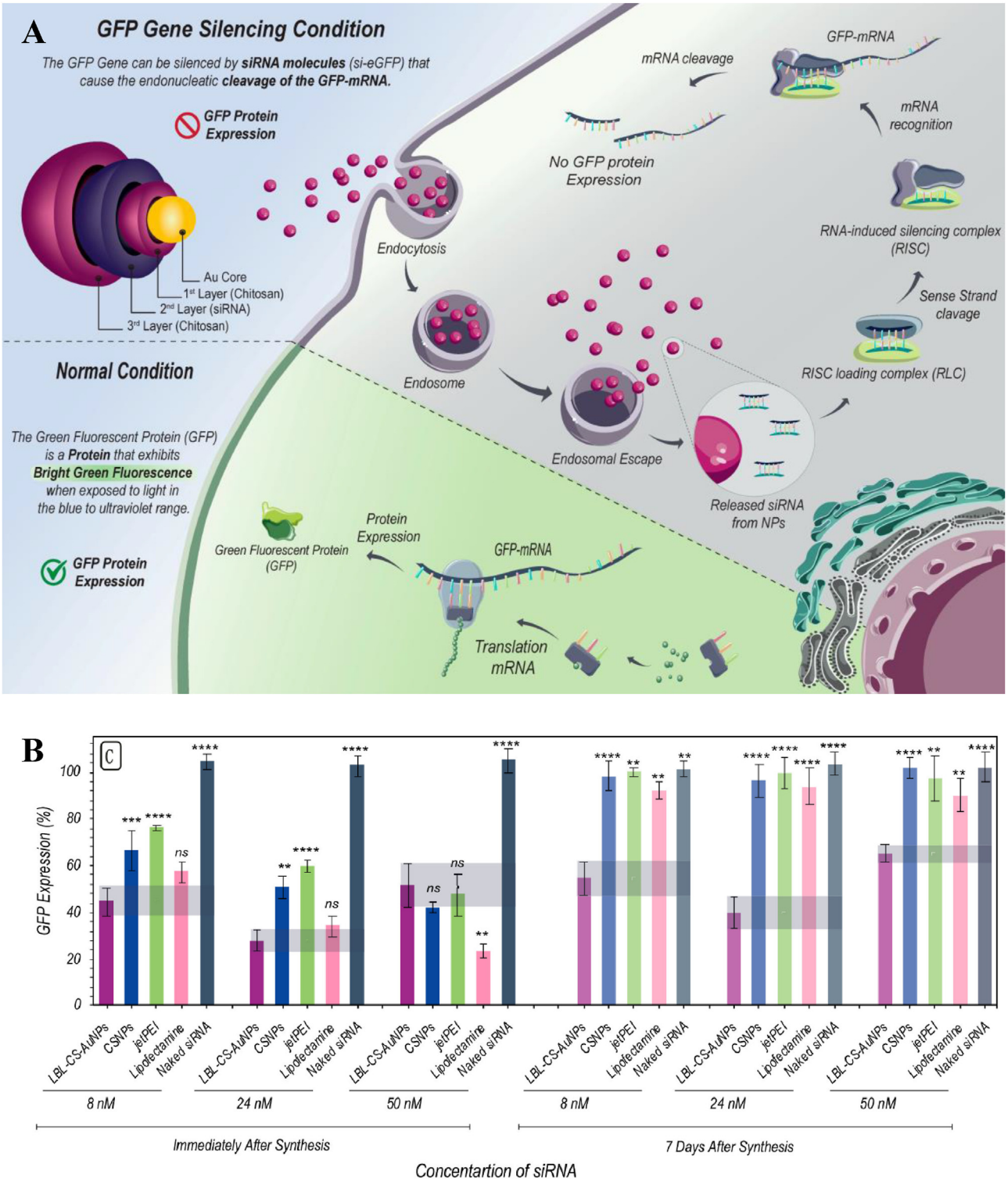

Fig. 6. (A) Schematic representation of LBL-CS-AuNPs for siRNA delivery. (B) Evaluation of the knockdown efficacy of LBL-CS-AuNPs [46].

prediction of Alzheimer's disease [51]. Human brain endothelial cells (HBEC-5i) were used to show their biological safety on healthy cells, giving biomedical experts confidence in utilizing AuNPs for neurodegenerative disease control.

Spherical nucleic acids (SNAs), consisting of an AuNP core and a layer of aggregated oligonucleotides to ensure the efficiency of nucleic acid carriage, were used for effective treatment of amyotrophic lateral sclerosis [52]. SiRNAs at a 10% molar ratio to

polymer molecules were utilized to study the delivering efficiency. The nanocarrier provided advantages of sequence-specific loading, nuclease resistance and controllable manipulation of receptor-mediated endocytosis. Nevertheless, major hindrances lied in accumulation in endosomal pathway and vulnerability to lysosomal degradation. In order to overcome these challenges, SNA were further designed to conjugate with a diblock copolymer $PMPC_{25}$—$PDPA_{72}$. The copolymer benefited siRNA delivery with its intrinsic ability to escape from endosomal pathway, warranting safe carriage to cytosol. When compared to lipofectamine, the copolymer modified SNA nanocarrier with doses three orders of magnitude lower provides comparable knockdown effect of C9orf72. AuNPs modified with positively charged Tat-related cell-penetrating peptide were used as a satisfactory vector for siRNA delivery to retinal pigment epithelial cells [53]. The optimal ratio found between siRNA and AuNPs was 1:40. The nanocarrier successfully deliver the siRNA to ARPE-19 cells without loss of biological activity, leading to an efficient knockdown effect on cell production activated by secreted embryonic alkaline phosphatase. To tackle the difficulties in vascularization and wound healing induced by prostaglandin transporter (PGT) gene overexpression in patients with hyperglycemia, dicer substrate siRNA (DsiRNA) and AuNPs were co-loaded into PF127 gel [54]. Approximately 1 mL of DsiRNA against the prostaglandin transporter gene (0.015 mg/mL) was added to produce DsiRNA-loaded AuNPs. In the rat treated with the functional gel, more rapid wound closure was revealed. In addition, it provided higher levels of prostaglandin E2 and vascular endothelial growth factor (VEGF), revealing its capability to promote PGE2 production and angiogenesis. Epithelial cell adhesion molecule antibody conjugated AuNSs were shown to be valuable in site-specific intracellular delivery of fluorescent BLOCK-iT siRNA and GFP-encoding mRNA to specific ocular cells [55]. The cells were incubated with a fresh medium containing 0.5×10^{-6} M of VEGF-siRNA. Under photo irradiation, efficient thermal accumulation was generated around the functional AuNSs for boosting siRNA internalization. With optimal pulse fluence and scanning velocity, selective internalization of siRNA into ARE-19 cells was achieved.

3.2. Delivery of DNAs

Due to the COVID-19 pandemic caused by SARS-CoV-2, effective vaccines capable of inducing long-lasting immunity against SARS-CoV-2 variants have been the cornerstone of disease control. DNA vaccines encoding the S protein of SARS-CoV-2 were explored for their potential of immunization through intranasal administration [56]. AuNSs modified with chitosan, with the ability to potentiate vaccine immunogenicity and effectiveness, were designed as a nanocarrier for transporting DNA vaccines. 2 μg of DNA was encapsulated to estimate loading capacity of AuNSs. The immune response to intranasal delivery was remarkable based on continuous elevation of antibody level and neutralization of pseudoviruses expressing S proteins. AuNSs-chitosan was found to be a novel nanoformulation delivering DNAs and stabilizing nucleic acids. The entry of SARS-CoV-2 and its variants was effectively prohibited by high levels of anti-SC2 IgA acquired in lung mucosa and tissue-resident memory T cells, with immunity lasting for several weeks.

Delivery of DNA with porous shaped AuNPs (gold nanocages) conjugated with lactoferrin and diaminobutyric polypropylenimine dendrimer was demonstrated for treating prostate cancer [57]. The weight ratios of DAB-Lf: DNA ranged from 0.5:1 to 40:1, with DNA concentration maintained at 1 μg/mL. The modified nanocage further complexed with a plasmid DNA to form a DNA nanocarrier showed its potential to enhance gene expression and suppress cell proliferation in PC-3 prostate cancer cells. The complexed DNA could disassociate from gold conjugates more easily following internalization by the cell. In addition, TNFα encoded by the nanocarrier presented anti-proliferative activity 9-fold higher than that encoded by DAB dendriplex, showing its potential in future prostate cancer therapy.

Since multidrug-resistant (MDR) bacterial infections have aroused great interest among clinical caregivers and become a major issue in medical field, effective treatment against methicillin-resistant *Staphylococcus aureus* (MRSA) seems to be the building blocks of MRSA infection management. Antisense oligonucleotides (ASOs) carried by a multilayer coated AuNPs functionalized with PEI showed specificity to target mecA gene [58]. The initial loading concentration of ASOs was 100 μM. The nanovector was successfully internalized into MRSA and caused a 74% silencing of the mecA gene expression with high selectivity. Efficient internalization of other Gram-positive bacteria such as *Staphylococcus epidermidis* and *Bacillus subtilis* was also witnessed, with enhanced resistance to nuclease degradation. Suppression of MRSA bacteria growth (~71%) was achieved using oxacillin with the help of the nanovector, indicating restoration of bacterial sensitivity.

Telomerase is a ribonucleoprotein polymerase that is often found in cancer tissues but absent in normal ones. Thus, developing oligonucleotide inhibitors of telomerase may be an effective approach to control cancerous diseases. However, a major challenge for this approach lies in poor cellular uptake. AuNPs decorated with two oligonucleotides (one is complementary to the telomerase RNA template subunit and the other one conjugated to diethylenetriamine pentaacetate for radiolabeling with $InCl_3$), PEG, and cell-penetrating peptide Tat were used in the investigation of synchronizing telomerase inhibition [59]. The concentration of oligonucleotides used for the investigation was 1.5 μM. Cellular uptake of radiolabeled oligonucleotides was promoted without loss of its potential for telomerase inhibition. Resistance to endonuclease degradation was also significantly improved, promising safe delivery of oligonucleotides. Clonogenic survival of telomerase-positive cells experienced a dose-dependent reduction, which was not observed with telomerase-negative cells. Sensitizing cancer cells emitting radiation was achieved after successful delivery of radiolabeled oligonucleotides into cancer cells, which may boost further progress in AuNPs-based radiopharmaceuticals.

AuNRs conjugated with poly(amidoamine) dendrimers (PAMAM, G3) and GX1 peptide that is specific for tumor targeting were synthesized to deliver FAM172A under laser irradiation to colon cancer cells HCT-8 [60]. The carrier delivered FAM172A to cancer cells with high specificity and transfection efficiency. To form the most stable complex and achieve the most efficient delivery, the weight ratios of the Au NR@PAMAM-GX1/FAM172A ranged between 10:1 and 50:1. The viability of the HCT-8 cells treated with the FAM172A loaded delivery platform was significantly lower than that of the ones treated with single-mode phototherapy or gene therapy. Positively charged nanocomplex reduced the resistance to the FAM172A by negatively charged cell membrane and protected FAM172A from intracellular endonuclease degradation. Low cytotoxicity and ideal biocompatibility allowed it to be considered for an integrative treatment plan. The schematic illustration of FAM172A delivery and the experimental results are shown in Fig. 7.

4. Perspectives

The thriving evolution of incorporating AuNPs in quantitation and delivery of nucleic acids has drastically changed our viewpoints toward nanotechnology and marked a giant move in research of genomics. A plethora of strategies based on different structures of AuNPs have been corroborated to play crucial roles in quantitation and transport of nucleic acids in biological systems. Surface modification with multifarious materials and integration with diversified amplification techniques portray the infinity of advancement in AuNPs-mediated diagnosis and therapy for gene-related diseases. By taking advantages of ease in bioconjugation, biocompatibility, and stability, various functional AuNPs have been demonstrated with high sensitivity and specificity for quantitation of low levels of nucleic acids in complicated biological samples such as cells. AuNPs-NAA with high amplification efficiency are powerful for detection of nucleic acids in a single-cell level. Successful examples have shown that many functional AuNPs are efficient carriers for delivery of nucleic acids to specific targets such as cancer cells, viruses, wounded area, and tumors, showing their great future in gene therapy.

Nevertheless, there are still challenges ahead on the avenue to the matureness of AuNPs-based strategies. In the aspect of quantitation of nucleic acids, the precision and accuracy of detection may be time-dependent since the impacts of certain biomolecules conjugated to AuNPs are to be explored, which raised a question of feasibility in complex samples. Other factors such as binding strength between nucleic acids and AuNPs, pH value of the environment, immobilization density of nucleic acid probes on AuNPs surface also need to be thoroughly discussed since they may be influential on aggregation and conformation of AuNPs. Some methods demand more complicated fabrication process in order to achieve lower detection limit. For example, several factors such as amplification time/cycle, pH, temperature, and solution composition must be optimized to achieve high sensitivity when applying functional AuNPs-NAA. Although the cytotoxicity of AuNPs is low, their accumulation in animal body is another concern when conducting *in-vivo* studies. With respect to delivery of nucleic acids, synthesis of nanovector with reproducible protocols, assurance of surface properties of AuNPs, sustainable nucleic acid release from the surface of AuNPs, and intactness of delivered materials after reaching the target are all major concerns awaiting appropriate solutions. More challenging issues such as elicitation of immunity, loading capacity for effective treatment, and degradation after internalization hamper further progress. Although successful examples have shown their potential for delivery of nucleic acids in cells and animals, they are not ready for commercial

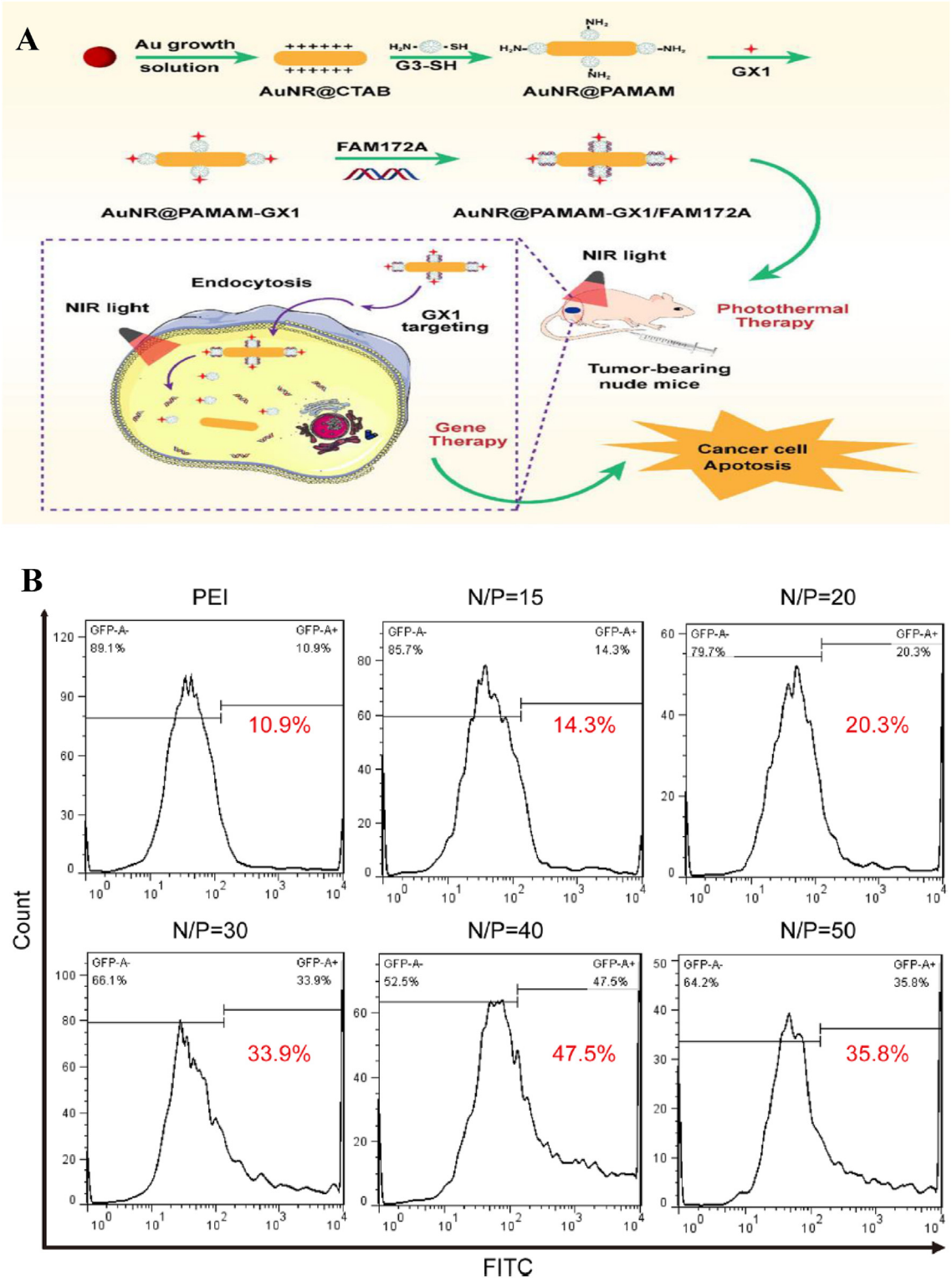

Fig. 7. (A) Schematic illustration of the GX1-targeting nanoparticles for combinational therapy for colon cancers treatment. (B) The gene transfection efficiency of the nanoplatform with different N/P ratios determined by flow cytometry [60].

use. Many issues such as tolerability, acceptable bioavailability, desired efficacy for targeted indications and understanding of the risk-benefit relationship in human bodies, are required to be carried out before functional AuNPs can be used safely for diseases treatment.

With regard to clinical translatability, potential limitations are also waiting to be overcome. Recent

clinical trials have shown significant progress in application of treatment for prevalent diseases like cancer, type I diabetes and neurodegenerative disorder and SARS-CoV2 immunization. Most clinical trials have completed their phase 0 and phase I studies, with the safety of AuNPs well-evaluated. Phase II and phase III studies, which are conducted for assessment of therapeutic efficacy, are usually before initiation or ongoing. Without results supporting further development, the scalability of clinical trials remains to be defined. The data may not be highly reproducible as certain conditions in materials synthesis are not fully controllable. Since the synthesis of AuNPs sensing and delivery platform is relatively inexpensive, performing the earlier phases of clinical trials generate much benefits for the research. However, as no clear evidence of efficacy, retention and clearance in human body has been observed, the cost-effectiveness in later phases is hard to calculate. The unspecified biodistribution and metabolism also set barriers for regulatory approvals and increase unpredictability in occurrence of adverse events.

In conclusion, although some of the AuNPs-assisted strategies are too miscellaneous and most of them are still far from clinical practice, they have already expanded the horizons of nanotechnology and redefined what's possible for quantitation and delivery of nucleic acids. It is believed that the current disadvantages will be addressed and AuNPs will continue to be meritorious nanomaterials with innovative discoveries that shine in the research of gene-related diseases.

Conflicts of interest

The authors announce that there are no competing financial interests or personal relationships influencing the work reported in this paper.

Acknowledgment

We gratefully acknowledge the support of the National Science and Technology Council of Taiwan (MOST 111-2113-M-037-010 and 110-2113-M-002-005-MY3) for the funding of this work.

References

[1] Wang CC, Wu SM, Li HW, Chang HT. Biomedical applications of DNA-conjugated gold nanoparticles. Chembiochem 2016;17:1052–62. https://doi.org/10.1002/cbic.201600014.
[2] Xie M, Jiang J, Chao J. DNA-based gold nanoparticle assemblies: from structure constructions to sensing applications. Sensors 2023;23:9229. https://doi.org/10.3390/s23229229.
[3] Ma XY, Li XQ, Luo GY, Jiao J. DNA-functionalized AuNPs: modification, characterization, and biomedical applications. Front Chem 2022;10:1095488. https://doi.org/10.3389/fchem.2022.1095488.
[4] Huang CC, Chiang CK, Lin ZH, Lee KH, Chang HT. Bioconjugated gold nanodots and nanoparticles for protein assays based on photoluminescence quenching. Anal Chem 2008;80:1497–504. https://doi.org/10.1021/ac701998f.
[5] Shiang YC, Hsu CL, Huang CC, Chang HT. Gold nanoparticles presenting hybridized self-assembled aptamers that exhibit enhanced inhibition of thrombin. Angew Chem Int Ed 2011;50:7660–5. https://doi.org/10.1002/anie.201101718.
[6] Kesharwani P, Ma R, Sang L, Fatima M, Sheikh A, Abourehab MAS, et al. Gold nanoparticles and gold nanorods in the landscape of cancer therapy. Mol Cancer 2023;22:98. https://doi.org/10.1186/s12943-023-01798-8.
[7] Yañez-Aulestia A, Gupta NK, Hernández M, Osorio-Toribio G, Sánchez-Gonzalez E, Guzmán-Vargas A, et al. AuNPs: current and upcoming biomedical applications in sensing, drug, and gene delivery. Chem Commun 2022;58:10886. https://doi.org/10.1039/D2CC04826D.
[8] Guimarães D, Cavaco-Paulo A, Nogueira E. Design of liposomes as drug delivery system for therapeutic applications. Int J Pharm 2021;601:120571. https://doi.org/10.1016/j.ijpharm.2021.120571.
[9] Ferrari E. Gold nanoparticle-based plasmonic biosensors. Biosensors 2023;13:411. https://doi.org/10.3390/bios13030411.
[10] Karami A, Hasani M, Jalilian FA, Ezati R. Conventional PCR assisted single-component assembly of spherical nucleic acids for simple colorimetric detection of SARS-CoV-2. Sens Actuator B-Chem 2021;328:128971. https://doi.org/10.1016/j.snb.2020.128971.
[11] Jiang YZ, Hu ML, Liu AA, Lin Y, Liu LL, Yu B, et al. Detection of SARS-CoV-2 by CRISPR/Cas12a-Enhanced colorimetry. ACS Sens 2021;6:1086–93. https://doi.org/10.1021/acssensors.0c02365.
[12] Liu L, Xiong HJ, Wang XM, Jiang H. Gold nanomaterials: important vectors in biosensing of breast cancer biomarkers. Anal Bioanal Chem 2024. https://doi.org/10.1007/s00216-024-05151-w (in press).
[13] Jahangiri-Manesh A, Mousazadeh M, Taji S, Bahmani A, Zarepour A, Zarrabi A, et al. Gold nanorods for drug and gene delivery: an overview of recent advancements. Pharmaceutics 2022;14:664. https://doi.org/10.3390/pharmaceutics14030664.
[14] Kanu GA, Parambath JBM, Odeh RO, Mohamed AA. Gold nanoparticle-mediated gene therapy. Cancers 2022;14:5366. https://doi.org/10.3390/cancers14215366.
[15] Entezari M, Abad GGY, Sedghi B, Ettehadi R, Asadi S, Beiranvand R, et al. Gold nanostructure-mediated delivery of anticancer agents: biomedical applications, reversing drug resistance, and stimuli-responsive nanocarriers. Environ Res 2023;255:115673. https://doi.org/10.1016/j.envres.2023.115673.
[16] Zhu S, Yang YQ, Ding Yd, Feng NH, Li MG. YinYM. Engineering entropy-driven based multiple signal amplification strategy for visualized assay of miRNA by naked eye. Talanta 2021;235:122810. https://doi.org/10.1016/j.talanta.2021.122810.
[17] Chai H, Chen XF, Shi RJ, Miao P. Irregular DNA triangular prism/triplex assembly for duplicate miRNA analysis with nicking endonuclease-mediated amplification. Anal Chem 2023;95:4564–9. https://doi.org/10.1021/acs.analchem.3c00087.
[18] Xu YJ, Da JJ, Lan Q, Luo J, Lu ZS, Peng R, et al. Engineering DNA tetrahedron as a sensing surface of lateral flow test strips and ratiometric visual detection of exosomal microRNA-150–5p. Sens Actuator B-Chem 2023;393:134266. https://doi.org/10.1016/j.snb.2023.134266.
[19] Kong LY, Lv S, Qiao ZJ, Yan YC, Zhang J, Bi S. Metal-organic framework nanoreactor-based electrochemical biosensor coupled with three-dimensional DNA walker for label-free detection of microRNA. Biosens Bioelectron 2022;207:114188. https://doi.org/10.1016/j.bios.2022.114188.
[20] Hou YY, Xie WZ, Huang KJ, Xu J. AuNPs/graphdiyne self-powered sensing platform for sensitive detection of microRNA with DNAzyme walker for signal amplification. Anal Chim Acta 2023;1240:340754. https://doi.org/10.1016/j.aca.2022.340754.

[21] Wang X, Sun HZ, Liu BJ, Jiang KM, Li ZH, Meng HM. DNA dendrimer-based directed 3D walking nanomachine for the sensitive detection and intracellular imaging of miRNA. Anal Chem 2022;94:17232–9. https://doi.org/10.1021/acs.analchem.2c03963.
[22] Zhang X, Wei X, Qi JJ, Shen J, Xu JW, Gong GY, et al. Simultaneous detection of bladder cancer exosomal MicroRNAs based on inorganic nanoflare and DNAzyme walker. Anal Chem 2022;94:4787–93. https://doi.org/10.1021/acs.analchem.1c05588.
[23] Wang YH, Shao ZS, Cheng C, Wang JL, Song Z, Song WJ, et al. Fluorescent oligonucleotide indicators for ratiometric microRNA sensing onmetal-organic frameworks. Chem Eng J 2022;437:135296. https://doi.org/10.1016/j.cej.2022.135296.
[24] Xu HM, Zhang ZZ, Wang YH, Zhang XM, Zhu JJ, Min QH. Sense and validate: fluorophore/mass dual-encoded nanoprobes for fluorescence imaging and MS quantification of intracellular multiple MicroRNAs. Anal Chem 2022;94:6329–37. https://doi.org/10.1021/acs.analchem.2c00513.
[25] Tripathi A, Jain R, Dandekar P. Rapid visual detection of Mycobacterium tuberculosis DNA using gold nanoparticles. Anal Methods 2023;15:2497–504. https://doi.org/10.1039/d3ay00195d.
[26] Pei XJ, Hong H, Liu ST, Li N. Nucleic acids detection for Mycobacterium tuberculosis based on gold nanoparticles counting and rolling-circle amplification. Biosensors 2022;12:448. https://doi.org/10.3390/bios12070448.
[27] Xu Y, Xiao GY, Chen BB, He M, Hu B. Single particle inductively coupled plasma mass spectrometry-based homogeneous detection of HBV DNA with rolling circle amplification-induced gold nanoparticle agglomeration. Anal Chem 2022;94:10011–8. https://doi.org/10.1021/acs.analchem.2c00272.
[28] Sivakumar R, Dinh VP, Lee NY. Ultraviolet-induced in situ gold nanoparticles for point-of-care testing of infectious diseases in loop-mediated isothermal amplification. Lab Chip 2021;21:700. https://doi.org/10.1039/D1LC00019E.
[29] Jiang XX, Yang MH, Liu JW. Capping gold nanoparticles to achieve a protein-like surface for loop-mediated isothermal amplification acceleration and ultrasensitive DNA detection. ACS Appl Mater Interfaces 2022;14:27666–74. https://doi.org/10.1021/acsami.2c06061.
[30] Ning W, Zhan CY, Tian ZY, Wu MF, Luo ZW, Hu SM, et al. Ω-shaped fiber optic LSPR biosensor based on mismatched hybridization chain reaction and gold nanoparticles for detection of circulating cell-free DNA. Biosens Bioelectron 2023;228:115175. https://doi.org/10.1016/j.bios.2023.115175.
[31] Carter E, Davis SA, Hill DJ. Rapid detection of Neisseria gonorrhoeae genomic DNA using gold nanoprobes which target the gonococcal DNA uptake sequence. Front Cell Infect Microbiol 2022;12:920447. https://doi.org/10.3389/fcimb.2022.920447.
[32] Zhang ZK, Shang CY, Hu CX, Liu YM, Han JL. Branched DNA-based electrochemical biosensor for sensitive nucleic acids analysis with gold nanoparticles as amplifier. Int J Mol Sci 2023;24:12565. https://doi.org/10.3390/ijms241612565.
[33] Yu QC, Zhang J, Qiu WW, Li K, Qian LS, Zhang XJ, et al. Gold nanorods-based lateral flow biosensors for sensitive detection of nucleic acids. Microchim Acta 2021;188:133. https://doi.org/10.1007/s00604-021-04788-z.
[34] Razmi N, Hasanzadeh M, Willander M, Nur O. Electrochemical genosensor based on gold nanostars for the detection of Escherichia coli O157:H7 DNA. Anal Methods 2022;14:1562. https://doi.org/10.1039/D2AY00056C.
[35] Anwar S, Khawar MB, Ovais M, Afzal A, Zhang X. Gold nanocubes based optical detection of HIV-1 DNA via surface enhanced Raman spectroscopy. J Pharm Biomed Anal 2023;226:115242. https://doi.org/10.1016/j.jpba.2023.115242.
[36] Zhang Y, Lyu XM, Chen DS, Wu J, Li DW, Li Y. DNA induced CTAB-caped gold bipyramidal nanoparticles self-assembly using for Raman detection of DNA molecules. Talanta 2024;266:124936. https://doi.org/10.1016/j.talanta.2023.124936.
[37] Chaudhari R, Nasra S, Meghani N, Kumar A. MiR-206 conjugated gold nanoparticle based targeted therapy in breast cancer cells. Sci Rep 2022;12:4713. https://doi.org/10.1038/s41598-022-08185-1.
[38] Guo WN, Wu ZJ, Chen JR, Guo S, You WM, Wang SJ, et al. Nanoparticle delivery of miR-21-3p sensitizes melanoma to anti-PD-1 immunotherapy by promoting ferroptosis. J Immunother Cancer 2022;10:e004381. https://doi.org/10.1136/jitc-2021-004381.
[39] Li CS, Li J, Fan Y, Wang DY, Zhan MS, Shen MW, et al. Co-Delivery of dexamethasone and a MicroRNA-155 inhibitor using dendrimer-entrapped gold nanoparticles for acute lung injury therapy. Biomacromolecules 2021;22:5108–17. https://doi.org/10.1021/acs.biomac.1c01081.
[40] Peng JF, Wang RR, Sun WR, Huang MH, Wang R, Li YJ, et al. Delivery of miR-320a-3p by gold nanoparticles combined with photothermal therapy for directly targeting Sp1 in lung cancer. Biomater Sci 2021;9:6528. https://doi.org/10.1039/D1BM01124C.
[41] Mbatha LS, Maiyo F, Daniels A, Singh M. Dendrimer-coated gold nanoparticles for efficient folate-targeted mRNA delivery in vitro. Pharmaceutics 2021;13:900. https://doi.org/10.3390/pharmaceutics13060900.
[42] Gustà MF, Edel MJ, Salazar VA, Alvarez-Palomo B, Juan M, Broggini M, et al. Exploiting endocytosis for transfection of mRNA for cytoplasmatic delivery using cationic gold nanoparticles. Front Immunol 2023;14:1128582. https://doi.org/10.3389/fimmu.2023.1128582.
[43] Xue C, Hu SY, Gao ZH, Wang L, Luo MX, Yu X, et al. Programmably tiling rigidified DNA brick on gold nanoparticle as multi-functional shell for cancer targeted delivery of siRNAs. Nat Commun 2021;12:2928. https://doi.org/10.1038/s41467-021-23250-5.
[44] Abashkin V, Pedziwiatr-Werbicka E, Gómez R, Javier de la Mata F, Dzmitruk F, Shcharbin D, et al. Prospects of cationic carbosilane dendronized gold nanoparticles as non-viral vectors for delivery of anticancer siRNAs siBCL-xL and siMCL-1. Pharmaceutics 2021;13:1549. https://doi.org/10.3390/pharmaceutics13101549.
[45] Yu AYH, Fu RH, Hsu SH, Chiu CF, Fang WH, Yeh CA, et al. Epidermal growth factor receptors siRNA-conjugated collagen modified gold nanoparticles for targeted imaging and therapy of lung cancer. Mater Today Adv 2021;12:100191. https://doi.org/10.1016/j.mtadv.2021.100191.
[46] Shaabani E, Sharifiaghdam M, Keersmaecker HD, Rycke RD, Smedt SD, Faridi-Majidi R, et al. Layer by layer assembled chitosan-coated gold nanoparticles for enhanced siRNA delivery and silencing. Int J Mol Sci 2021;22:831. https://doi.org/10.3390/ijms22020831.
[47] Minassian G, Ghanem E, Hage RE, Rahme K. Gold nanoparticles conjugated with Dendrigraft poly-L-lysine and folate-targeted poly(ethylene glycol) for siRNA delivery to prostate cancer. Nanotheranostics 2023;7:152–66. https://doi.org/10.7150/ntno.79050.
[48] Chen S, Li JG, Ma XY, Liu F, Yan GP. Cationic peptide-modified gold nanostars as efficient delivery platform for RNA interference antitumor therapy. Polymers 2021;13:3764. https://doi.org/10.3390/polym13213764.
[49] Chakraborty K, Biswas A, Mishra S, Mallick AM, Tripathi A, Jan S, et al. Harnessing peptide-functionalized multivalent gold nanorods for promoting enhanced gene silencing and managing breast cancer metastasis. ACS Appl Bio Mater 2023;6:458–72. https://doi.org/10.1021/acsabm.2c00726.
[50] Zhang M, Lin JT, Jin JK, Yu W, Qi YY, Tao HM. Delivery of siRNA using functionalized gold nanorods enhances anti-osteosarcoma efficacy. Front Pharmacol 2021;12:799588. https://doi.org/10.3389/fphar.2021.799588.
[51] Okła E, Białecki P, Kedzierska M, Pedziwiatr-Werbicka E, Miłowska K, Takvor S, et al. Pegylated gold nanoparticles conjugated with siRNA: complexes formation and cytotoxicity. Int J Mol Sci 2023;24:6638. https://doi.org/10.3390/ijms24076638.

[52] Garcia-Guerra A, Ellerington R, Gaitzsch J, Bath J, Kye M, Varela MA, et al. A modular RNA delivery system comprising spherical nucleic acids built on endosome escaping polymeric nanoparticles. Nanoscale Adv 2023;5: 2941. https://doi.org/10.1039/D2NA00846G.

[53] Elizarova TN, Antopolsky ML, Novichikhin DN, Skirda AM, Orlov AV, Bragina VA, et al. A straightforward method for the development of positively charged gold nanoparticle-based vectors for effective siRNA delivery. Molecules 2023; 28:3318. https://doi.org/10.3390/molecules28083318.

[54] Azlan AYHN, Katas H, Zin NM, Fauzi MB. Dual action gels containing DsiRNA loaded gold nanoparticles: augmenting diabetic wound healing by promoting angiogenesis and inhibiting infection. Eur J Pharm Biopharm 2021;169:78–90. https://doi.org/10.1016/j.ejpb.2021.09.007.

[55] Kafshgari MH, Agiotis L, Largillière I, Patskovsky S, Meunier M. Antibody-functionalized gold nanostar-mediated on-resonance picosecond laser optoporation for targeted delivery of RNA therapeutics. Small 2021;17:2007577. https://doi.org/10.1002/smll.202007577.

[56] Kumar US, Afjei R, Ferrara K, Massoud TF, Paulmurugan R. Gold-nanostar-chitosan-mediated delivery of SARS-CoV-2 DNA vaccine for respiratory mucosal immunization: development and proof-of-principle. ACS Nano 2021;15: 17582–601. https://doi.org/10.1021/acsnano.1c05002.

[57] Almowalad J, Laskar P, Somani S, Meewan J, Tate RJ, Dufès C. Lactoferrin- and dendrimer-bearing gold nanocages for stimulus-free DNA delivery to prostate cancer cells. Int J Nanomed 2022;17:1409–21. https://doi.org/10.2147/IJN.S347574.

[58] Beha MJ, Ryu JS, Kim YS, Chung HJ. Delivery of antisense oligonucleotides using multi-layer coated gold nanoparticles to methicillin-resistant *S. aureus* for combinatorial treatment. Mater Sci Eng C 2021;126:112167. https://doi.org/10.1016/j.msec.2021.112167.

[59] Bavelaar BM, Song L, Jackson MR, Able S, Tietz O, Skaripa-Koukelli I, et al. Oligonucleotide-functionalized gold nanoparticles for synchronous telomerase inhibition, radiosensitization, and delivery of theranostic radionuclides. Mol Pharm 2021;18:3820–31. https://doi.org/10.1021/acs.molpharmaceut.1c00442.

[60] Ye LL, Chen YM, Mao JZ, Lei XT, Yang Q, Cui CH. Dendrimer-modified gold nanorods as a platform for combinational gene therapy and photothermal therapy of tumors. J Exp Clin Cancer Res 2021;40:303. https://doi.org/10.1186/s13046-021-02105-3.